www.mecsj.com

Multi-Knowledge Electronic Comprehensive Journal For
Education And Science Publications (MECSJ)
Issue (50) 2022
ISSN: 2616-9185

Performance Evaluation of Scalograms and 1-D Wavelet EEG Classifiers for Prosthetic Control System Optimisation

Amer Al-Canaan
Renewable Energy Department, Jadara University
Irbid, Jordan
Amer.Al-Canaan@USherbrooke.ca

and

Hicham Chakib
Electrical and Computer Engineering Department, University of Sherbrooke
Sherbrooke, Canada
Hicham.Chakib@USherbrooke.ca

Abstract

Electroencephalography (EEG) is utilised to analyse faint brain signals, which vary in amplitude and frequency depending on brain state during emotions, movement and motor effects. EEG and Brain-Computer Interface (BCI) technology combined with machine learning is deployed in prosthesis control to help amputee and people suffering from severe injuries. In this work, we utilise the Wavelet Transform (WT) to extract EEG features for optimal prosthetic arm control. Unlike most of research work, our work is based upon high-resolution EEG data set (with 2-kHz sampling frequency), dual-channel EEG acquisition module and large-size scalograms, which accounts for the need of data augmentation techniques necessary in deep learning models. We present our results of performance evaluation of 1-D and scalograms classifiers for optimal prosthetic BCI arm control system. We designed our optimal control system using five 1-D Wavelet classifiers including Linear Discriminant Analysing (LDA) and Multi-Layer Perceptron (MLP) as well as 2-D representations of EEG signals (scalograms). The EEG data set was accumulated with the help of 7 subjects who performed 4 different mental activities during each recording session. Each mental activity was recorded during 8 seconds using a dual-channel EEG acquisition module, which was set up at 2 kHz sampling frequency. The scalograms are generated during training using resampled EEG data at 500 Hz, which produced scalograms with sizes of 1500×300 pixels.

Our performance evaluation results showed high training and testing accuracies for 1-D Wavelet classifiers and scalograms as well. The optimisation results have shown that with the scalograms and 2-D CNN classifier the optimal performance was determined (where training accuracy was 98%) after discarding 2 seconds of the 8-second EEG data and resizing the resulting scalograms to 22% of their maximum size. On the other hand, 1-D Wavelet classifiers showed optimal performance with 95% training accuracy and trimming of 4 seconds. The overall performance of 1-D Wavelet classifiers, MLP in particular, is advantageous in the context of prosthetic arm control due to the high training speed and reduction of EEG data length by half (4 seconds).

The complete designed system consists of EEG acquisition, BCI and control modules hosted in a raspberry pi 4, single-board computer system. The designed BCI control system is operated through a comprehensive Graphical User Interface (GUI) using Python.

Our contribution in this field include the design of an optimal BCI prosthetic arm control system with emphasis on wide-bandwidth EEG data set, low number of EEG channels, high accuracy and affordable processing hardware of raspberry pi 4. The application of the designed performance optimisation procedure for prosthetic arm control is beneficial to other similar BCI applications.

Key words : EEG, Wavelets, Deep learning, Prosthetic arm control

1 Introduction

Brain-Computer Interface (BCI) combined with scalograms classifiers enable direct generation of control signal using Electroencephalography (EEG) signals [32] that are analysed during different brain states including emotion recognition using speech analysis with Wavelets [15]. BCI technology is employed in many domains including biomedical applications, prosthesis control for instance, to help people with certain disabilities [26]. Hands-free applications are one typical example where BCI research became involved [32, 26, 1, 33, 8]. Other BCI research domains include industry, education, advertising, entertainment, and smart transportation [8].

BCI research is challenging due to various reasons, such as user acceptance and technical development. People with motor disabilities could gain the ability to express themselves, to write down their opinions due to BCI-based projects, such as prostheses control, spelling applications [21], semantic categorisation [34], or silent speech communication [8].

In section 1.1, we present our contributions. A brief discussion of brain waves is in 1.2. Electrodes and montage are presented in 1.3. EEG artefacts are discussed

www.mecsj.com
Multi-Knowledge Electronic Comprehensive Journal For Education And Science Publications (MECSJ)
Issue (50) 2022
ISSN: 2616-9185

in 1.4. In section 2, we present related work and design methodology in section 3. Discussion of results is presented in section 4. Conclusion and future work is in section 5.

1.1 Contributions

In this work, we present our contributions, which can be summarised as follows:

1. Evaluate the performance of scalograms in CNN classifiers (with both *rgb* and *grayscale* modes) and 1-D Wavelet classifiers in the context of optimising prosthetic BCI control system.

2. We promote the utilisation of relatively wide bandwidth EEG input data set in order to increase the accuracy of classification. Our designed classifier models depend upon high-resolution EEG data set with sampling frequency of 2 kHz and relatively high bandwidth of 500 Hz in order to optimise training and testing accuracies. The EEG data set utilised in this work was provided by a dual-channel EEG acquisition module from previous work [2].

3. We present comparison between 2 types of Wavelet classifiers, namely, and various 1-D EEG classifiers, which are used to optimise the length of EEG data and classifier model parameters. Our results have shown that the EEG data can be shortened by 4 seconds when 1-D classifiers are utilised and by 2 seconds when the designed scalograms CNN is utilised. This corresponds to EEG data length of 4 seconds and 6 seconds, for 1-D classifiers and scalograms, respectively. On the other hand, our experimentations have shown that optimal resize parameter for the scalograms CNN classifier model was 22%. This has significantly reduced training time and processing resources to accomplish model training and testing.

4. Design of a compact EEG control system for prosthetic arm, which is hosted on raspberry pi 4. All modules except for the analogue EEG acquisition modules are hosted on raspberry pi with 8 GHz memory. The complete system is operated through a GUI, which trains different EEG classifiers and loads trained models for actual operation on live EEG data.

www.mecsj.com
Multi-Knowledge Electronic Comprehensive Journal For Education And Science Publications (MECSJ)
Issue (50) 2022
ISSN: 2616-9185

1.2 Brain Waves

Brain waves are low-magnitude complex electro-magnetic signals that can be measured using three methods that can be described as follows:

1. Electroencephalography (EEG), which enables recording of electrical brain signals, as shown in figures Figure 1 [26], that are as low as 0.1 μV using dry electrodes as shown in Figure 2 [25]. Electrodes are fixed on elastic ribbon headset to ease recording of electrical activity of the brain along the front lobe by measuring voltage fluctuations accompanying neuro-transmission activity within the brain [26]. The headset is easy to wear and use, though the resulting Signal-to-Noise Ratio (SNR) is low. Although invasive EEG produces higher signal level compared to non-invasive EEG, invasive techniques require complex surgery and thus are not considered in BCI systems. In this work, brain waves were provided using a dual-channel EEG acquisition module with bandwidth of 1000 Hz [2]. Deep sleep and drowsiness detection, for instance, can be achieved by analysing the lower frequency bands, while the higher frequencies are related to substantial concentration and spiritual states of the brain.

2. Magneto-encephalography (MEG), which measures magnetic fields produced by electrical currents of the brain.

3. Functional Magnetic Resonance Imaging (fMRI), which is based upon detecting the changes in blood flow related to neural activity in the brain and provides a high spatial resolution and captures information from deep parts of the brain that cannot be gathered by electrical or magnetic measuring [26].

Brain waves have been categorised into five major frequency bands: δ, θ, α, β and γ, as shown on the 10-second EEG signal in Figure 1. Studies have shown that certain activities can be correlated with increased in power for specific frequency ranges. For example, drowsiness and fatigue signs can be related to an increase in the θ frequency band from 4 to 8 Hz. In this work, we have calculated features for EEG sub-bands spanning the whole bandwidth of our design, i.e., 500 Hz, which can be described as follows:

1. δ from 0.1 to 4 Hz divided into 2 sub-bands; δ_1 (0.1-2) and δ_2 (2-4) Hz.

2. θ from 4 to 8 Hz divided into 2 sub-bands; θ_1 (4-6) and θ_2 (6-8) Hz.

3. α from 8 to 13 Hz divided into 2 sub-bands; α_1 (8-11) and α_2 (11-13) Hz.

www.mecsj.com
Multi-Knowledge Electronic Comprehensive Journal For Education And Science Publications (MECSJ)
Issue (50) 2022
ISSN: 2616-9185

4. β from 13 to 30 Hz divided into 3 sub-bands; β_1 (13-19), β_2 (19-25) and β_3 (25-30) Hz.

5. γ from 30 to 500 Hz divided into 12 sub-bands; γ_1 (30-70), γ_2 (70-110), γ_3 (110-150), γ_4 (150-190), γ_5 (190-230), γ_6 (230-270), γ_7 (270-310), γ_8 (310-350), γ_9 (350-390), γ_{10} (390-430), γ_{11} (430-470) and γ_{12} (470-500) Hz.

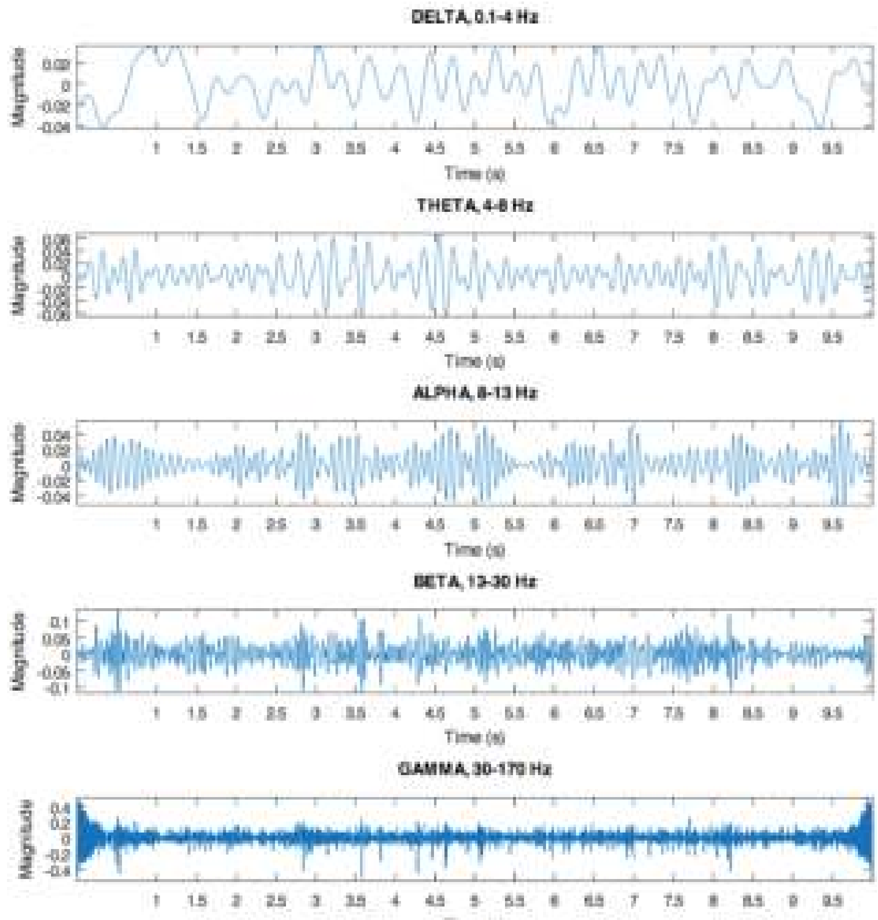

Figure 1: Example of EEG signal showing [2] its 5 frequency bands.

1.3 EEG Electrodes and montage

Electrodes are to maintain low electrical resistance with the scalp skin during EEG recording. Different types of electrodes are available for different applications, including disposable and reusable types. The disposable type was not considered in this context

Multi-Knowledge Electronic Comprehensive Journal For
Education And Science Publications (MECSJ)
Issue (50) 2022
ISSN: 2616-9185
www.mecsj.com

due to the high number of recordings needed to generate training and validation EEG data.

Reusable electrodes are more practical compared to wet electrodes [16] and can be utilised with or without gel. We have opted for the silver-plated cup electrodes, as shown in Figure 2 due to their durability and easy setup.

Our EEG acquisition system is based upon a dual-channel circuit [2] in order to fulfil design constraints related to versatility and ease of use. By using two channels only, the EEG acquisition module produces decent EEG signal quality that enables the classification module to achieve high accuracy. All EEG data were acquired using dry electrodes attached to a spongy ribbon placed on the forehead, as shown on Figure 3. The electrodes of both channels on the frontal lobe are placed according to the 10-20 system as follows: Channel 1: Differential input signal between Fp1 and Fp2 locations. Channel 2: Differential input signal between the left ear lobe and Fpz.

Figure 2: Silver-plated reusable EEG dry electrodes.

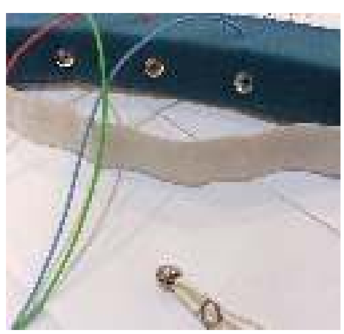

Figure 3: EEG headset with silver-cup electrodes fixed on elastic spongy ribbon.

www.mecsj.com
Multi-Knowledge Electronic Comprehensive Journal For Education And Science Publications (MECSJ)
Issue (50) 2022
ISSN: 2616-9185

1.4 EEG Artefacts

EEG artefacts describe undesired signals of non-cerebral origin. The amplitude of artefacts can be large relative to the size of amplitude of the cortical signals of interest. Some EEG artefacts are useful in various applications including Electro-occulography (EOG), which enables detecting and tracking eye-movements. EOG is important in Poly-somnography or sleep study, where it is used to diagnose sleep disorders, and is also used in EEG for assessing changes in alertness, drowsiness or sleep.

Power-line sources produce artefacts that can be attenuated by filtering out undesired power-line fundamental frequency and its harmonics between 0.2 and 500 Hz. In our context, band-stop (notch) filters are applied at both analogue and DSP modules to attenuate frequencies in a 60-Hz power system, i.e., 60, 120, 180 ... 480 Hz.

Band-pass filtering helps remove frequencies outside our intended range from 0.2 to 500 Hz. This is achieved by both the analogue acquisition module and digital filters, at the EEG acquisition and the pre-processing modules, respectively.

Other types of artefacts can be attenuated by smoothing algorithms, which is to remove outliers. The LowessSmoother algorithm from Python package tsmoothie was utilised to achieve this goal.

Experimental results have confirmed that the removal of artefacts improves the accuracy of the training and test for the different classifier models.

2 Related work

2.1 Medical applications of EEG, scalograms, deep learning and BCI

EEG and BCI are actively employed in various domains to overcome health issues [26], including prosthetic control for upper-limb amputee [35, 23], detection of tumour or cancer abnormal tissues [27, 28, 17], or certain brain disorders [13]. Mobile robots constitute another BCI application to help locked-in people to perform their daily activities [5]. BCI can be utilised to perform actions related to monitoring specific brain states, in particular, the perceived user emotional or cognitive state [30] or stress level [10, 31].

www.mecsj.com
Multi-Knowledge Electronic Comprehensive Journal For Education And Science Publications (MECSJ)
Issue (50) 2022
ISSN: 2616-9185

2.2 Neuroergonomics and smart environment

Smart homes and transportation benefit also from BCI and EEG technology by offering luxurious and commodity services. BCI-based is utilised in smart living environmental and auto-adjustment control systems [9, 24, 14].

Brain signals assist also in improving workplace conditions by assessment of an operator's cognitive state. They also help in analysing the impact of workload mental fatigue and task time on EEG features. Operating rooms are considered for smart workplace BCI-based applications, where the system measures the stress level of a surgeon and alerts according to the response type.

Intelligent transportation systems benefit also from BCI research as efficient and robust means to avoid accidents [12]. The work in [35] proposed a solution to help the amputee users perform precise finger movements. The problem is formulated as a Partially Observable Markov Decision Process. The optimal control policy was found by adaptive dynamic programming and reinforcement learning-based control algorithm-Deep Deterministic Policy Gradient combined with Hindsight Experience Replay.

The work in [29] uses a particle filtering based technique to infer user intent based on the trajectories of the user's hand by generating an estimation of the expected time left until reaching to an object, which is an essential variable in successful grasping of objects.

The authors in [19] used myoelectric pattern recognition systems to decode movement intention to drive upper-limb prostheses. The work is based upon Electromyography (EMG) by combining surface Electromyography (sEMG) with inertial measurements (IMs) and an appropriate training data collection paradigm. The results demonstrate that this can significantly improve classification performance as compared to conventional techniques exclusively based on sEMG signals. The work in [18] is also based upon EMG, where myoelectric prostheses allow users to recover lost functionality by controlling a robotic device with their remaining muscle activity.

Other research is being done on 3-D printed soft prosthetic hand control system [23] that is able to perform all the real-world grasping tasks, showing great potential in improving life quality of individuals with upper limb loss. In another work [22], 13 subjects were able to effectively control reaching of a robotic arm through modulation of their brain rhythms within the span of only a few training sessions.

The authors in [3] proposed an innovative low-cost five-fingered prosthetic hand that aims at enabling upper limb amputees to carry out their basic daily tasks more comfortably. A tendon-driven under actuated mechanism provides the necessary dexterity while keeping the mechanical and control complexity of the device low. The prosthetic is equipped with tactile sensors to improve the overall hand control. For the position control of each digit, a novel resistance feedback control scheme is devised and implemented. The design applied in provides a series of improvements in terms of size, weight and noise.

2-D and 3-D visual reshaping of EEG data are utilised as input to CNN classifiers, which produced accuracies ranging from 97.03% and 98.4% for 3 different data sets [6].

3 Design Methodology

This section provides design details of the prosthetic control system using Wavelets, which is shown in Figure 6.

3.1 Prosthesis with EEG control system structure

Prosthetic arm control faces usability challenges to have an efficient data acquisition, perform training session for volunteers and to conduct acquisition at various occasions and conditions on order to a provide coherent test results. Technical challenges include non-linearity, noise and non-stationary patterns of the brain signals. The block diagram of the designed BCI prosthetic control system (as shown on Figure 4 composed of several analogue and digital modules, which are described as follows [26]:

1. Analogue EEG signal acquisition. In invasive EEG acquisition, electrodes are implanted inside human body. Although this produces better SNR, it offers less flexibility and adds substantial complexity. Consequently, this method has very limited practical applications. Hence, non-invasive EEG acquisition is adopted in this work using dry electrodes that are attached to the frontal lobe using an elastic ribbon headset. This method offers more flexibility and requires signal conditioning and pre-processing to increase SNR.

2. Analogue signal conditioning and pre-processing. This module includes pre-amplification to increase SNR as well as analogue band-pass and notch filtering.

3. Digital Signal Processing (DSP). Analogue sensors capture various signal types, such as sound, light, temperature or pressure and prepare them for DSP modules. Analogue-to-Digital Converters (ADC) convert analogue signal into binary form ready for DSP, which sends back the processed signals to Digital-to-Analogue Converters (DAC), to their original form. Typical DSP modules suffer from high

www.mecsj.com
Multi-Knowledge Electronic Comprehensive Journal For Education And Science Publications (MECSJ)
Issue (50) 2022
ISSN: 2616-9185

power consumption, which can be overcome by the utilisation of FPGA modules. Many of the DSP modules are implemented efficiently with FPGA kits. Although FPGAs offer better performance than dedicated DSP kits, still FPGAs need a preliminary knowledge in Hardware Description Languages (HDL). In this work, DSP has to do with analysing and modifying digitised brain signals to achieve certain processing objectives such as filtering, artefact removal and smoothing. In this work, DSP employs various mathematical and computational algorithms on digital EEG signals to produce high-quality 1-D time series. DSP is also used to generate spectrograms and scalograms, i.e., 2-D representations of EEG signals, as shown on Figure 5.

4. Feature extraction. Relevant features include statistical calculations, 1-D Wavelet transforms and scalograms, which are 2-D representations of EEG signals using Wavelet transform [4], as shown in Figure 5. Wavelet features describe adequately EEG signals in time and frequency domains. The default Wavelet types utilised in this work include the Morlet (for scalograms) and Debauchies (for 1-D features). An example of scalograms is shown in Figure 5.

5. Classification. A classifier has the ability to distinguish new features after being trained using machine learning techniques, which include LDA, Quadrature Discriminant Analysis (QDA), Naïve Bayesian (NB), MLP and CNN. LDA projection is also used to reduce the number of relevant features in order to reduce processing and learning times.

6. Control module. The resulting classification output is fed into the control module in order to generate commands to the prosthetic hand, for instance.

The above first and second modules are deployed on dedicated EEG module board, while the other digital modules are deployed on raspberry pi 4, which is a single-board computer equipped with 8 GB memory, Ethernet, HDMI, USB and GPIO ports.

Two additional laptop computers have been utilised to perform multiple training sessions with different parameters to investigate optimal training models.

The hardware involved in the designed prosthetic arm control system is described as follows:

1. Headset with silver-cup dry electrodes, which maintain good electrical contact with the frontal lobe. The headset is composed of elastic ribbon and spongy piece to ensure easy and fast setup. The headset that we utilised is composed of two pairs of electrodes as shown on Figure 3.

www.mecsj.com
Multi-Knowledge Electronic Comprehensive Journal For Education And Science Publications (MECSJ)
Issue (50) 2022
ISSN: 2616-9185

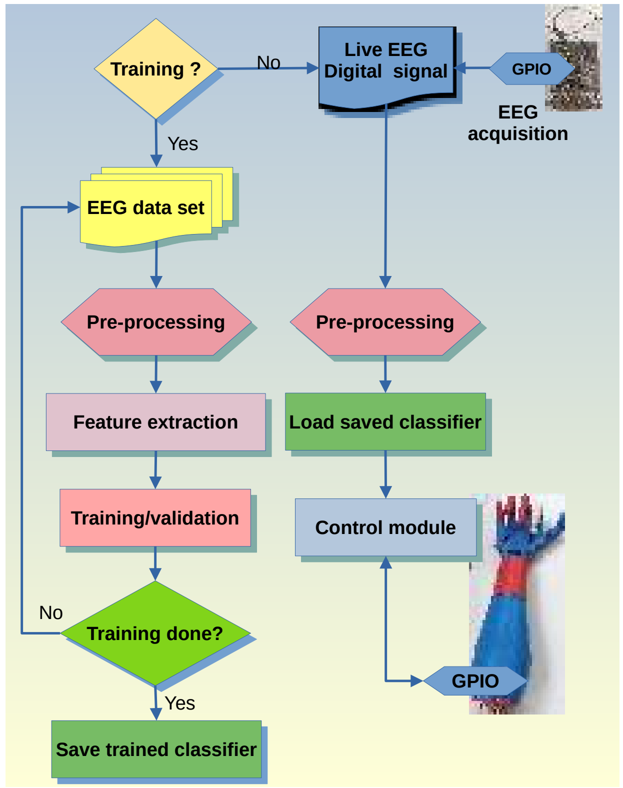

Figure 4: Block diagram of the BCI prosthetic arm control.

2. Analogue EEG acquisition. In this work, we utilised a dual-channel EEG acquisition circuit [2] that has analogue pre-filtering stage of 171-Hz, which is adequate for attenuating noise levels and prepare the EEG signal for subsequent digital filtering in the following DSP stage. The EEG acquisition module is connected with the EEG headset, the electronic explorer kit and the raspberry pi 4 through the GPIO pins. It captures, amplifies and filters brain signals that are converted into digital form using ADC during live capturing of EEG signals that are fed into the trained classifier. During recording sessions for training and

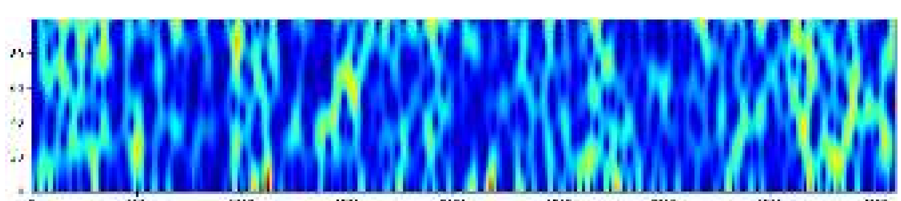

Figure 5: Scalograms of an EEG signal.

Multi-Knowledge Electronic Comprehensive Journal For
Education And Science Publications (MECSJ)
Issue (50) 2022
ISSN: 2616-9185
www.mecsj.com

testing data set, the EEG signal is fed into the Electronics Explorer board, which records 8 seconds of brain activity at a sampling frequency of 2 kHz.

3. Single-board computer (raspberry pi 4), which hosts the DSP, feature extraction, classification and control modules. The raspberry pi 4 include the feature extraction and classifier modules, which take digital input from the analogue EEG acquisition board and from the locally stored EEG data set. The control module is also hosted in the raspberry pi 4, which sends Pulse-Width Modulation (PWM) control signals to perform desired grip and wrist functions.

4. Electronics explorer board [11], which is a complete test bench equipped with several test modules including digital oscilloscope, function generator, DC source and multi-meter. This board was used to construct the EEG data set collected from recorded sessions at different sampling frequencies. The Electronics Explorer board is a useful measuring development kit that is also possible to be controlled and programmed by Python.

5. Prosthetic arm, which includes mechanical gears and embedded DC servomotors that take PWM control signals from the GPIO port of the raspberry pi 4 in order to generate the movements of the arm.

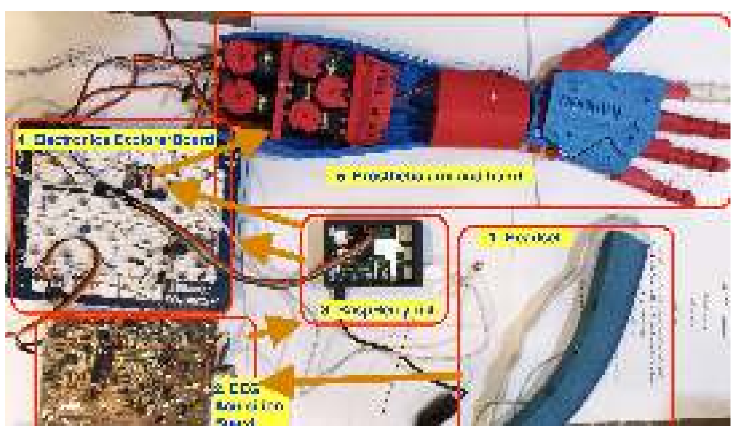

Figure 6: General overview of the prosthetic BCI control system.

3.2 DSP module using Python

We have utilised Python code to perform DSP that can be described as follows:

- filter unwanted power line noise including harmonics (60, 120, ..., 420, 480 Hz).

Multi-Knowledge Electronic Comprehensive Journal For
Education And Science Publications (MECSJ)
Issue (50) 2022
ISSN: 2616-9185
www.mecsj.com

- filter out signals outside EEG signals of interest within 0.2 and 500 Hz by using BPF, Finite Impulse Response Filter (FIR). The 500 Hz was chosen as a good compromise between accuracy and processing resources of the raspberry pi 4.
- generate EEG 1-D features by using statistical calculations as well as Wavelet transform.
- reduce the number of relevant statistical features using LDA in order to reduce processing time and memory.
- generate 2-D image representations of 1-D EEG signals using Wavelet scalograms, which are the input for the CNN classifier.

The main Graphical User Interface (GUI) of the EEG control system is shown in Figure 7, which is utilised to train the model and select the machine learning settings. Once training is done, the trained model is saved for the testing phase and for realistic operation of the prosthetic arm. The interface also accepts manual input off-line samples to be classified according to the trained model. Similarly, the live mode button allows direct EEG acquisition for actual operation by the user.

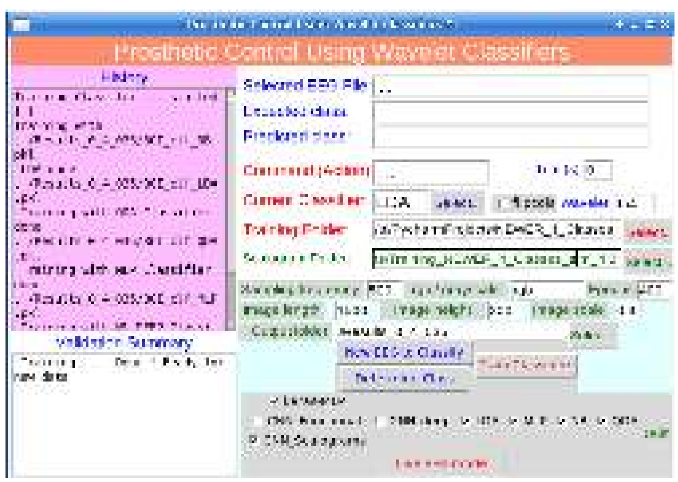

Figure 7: Main GUI of the prosthetic control modules.

3.3 EEG data set

Using the EEG acquisition module and the electronics explorer board, we have constructed a considerable data set with the participation of 7 male volunteers whose ages lie within 22 and 47 years. During recording sessions, each participant was

Multi-Knowledge Electronic Comprehensive Journal For Education And Science Publications (MECSJ)
Issue (50) 2022
ISSN: 2616-9185
www.mecsj.com

Table 1: Class labels for the EEG data set.

Class	Labels	Samples
1	Imagine moving right arm	48
2	Imagine grabbing an object with one hand	49
3	Using Whats-app application	44
4	Engage in a mobile telephone conversation	43

asked to perform 4 different physical gestures and mental exercise, two of which are pure brain activity (thinking or imagination) and the other two are mixed activities (brain and muscle) interaction. All of the 4 brain activities (classes) are described in table 1.

EEG data collection lasted for more than one year. All recordings were labelled with relevant information including the state of the participant (normal or drowsy), gesture description, participant name and serial number. The EEG data set includes more than 1000 recordings of 8-second durations. In this work we concentrate on a subset of our EEG data set that includes 184 recordings distributed over 4 classes. The presence of two channels for EEG data acquisition and the wide bandwidth of our EEG data (sampled at 2 kHz) has resulted in high training and testing accuracies, which eliminated the need for data augmentation [7].

3.4 Prosthetic arm

The prosthetic arm shown on Figure 6 was built using 3-D open-source printed [20]. The prosthetic arm can simulate different wrist and hand movements using 6 servomotors; 5 for the fingers and one for the wrist. The motors are connected to an external 5 V DC power source. The control module hosted on the raspberry pi 4 generates the PWM control signals related to each detected class.

4 Machine-learning results

Wavelet transform characterises EEG signals in terms of time and in frequency, therefore Wavelet features are calculated for 1-D EEG time series as well as 2-D scalograms (images). We have successfully integrated different types of feature classification models, such as LDA, QDA, NB, MLP and CNN, which can be selected for training using the GUI shown in Figure 7. The GUI also enables trimming the total recording period (8 seconds) as well as selecting various parameters for the scalograms including the colour mode (grayscale or rgb), the size of scalograms,

Multi-Knowledge Electronic Comprehensive Journal For
Education And Science Publications (MECSJ)
Issue (50) 2022
ISSN: 2616-9185
www.mecsj.com

Wavelet type and resampling frequency for the generation of scalograms. In rgb colour mode, scalograms use 8 bits per colour encoded from 0 to 255. Our experiments have shown that although CNN classifier with grayscale scalograms were faster in training, they were inferior in training accuracy compared to rgb mode, therefore we opted for the colour mode in subsequent experimentation.

Depending on the selected parameters, the training of deep learning classifiers, in particular, CNN with scalograms may be accomplished after 2-24 hours. Therefore, we performed experiments to study the effect of trimming the input EEG data and resizing the 2-D scalograms. The performances of 4 1-D Wavelet classifiers are shown in Figure 8 for NB, MLP (with sklearn Python library), LDA and keras-MLP classifiers. The testing curve for QDA is inferior to other classifier models.

The scalograms CNN performance varies with respect to trimming (between 0 and 7 seconds) the EEG data as shown in Figure 8. We assume that best performance is obtained when average training and validation (test) curves intersect (equal at a certain trimming point) or at least so close to each other. The MLP model (using sklearn library) and NB classifiers performed best compared to the others at trim of 4 seconds (corresponds to EEG data length of 4 seconds), where the training and validation curves are equal for LDA with accuracy of 97.0%. With trim of 1 second, the performance of LDA is best since the under fitting represented by the difference between training and validation curves is minimum, i.e., 1.39%. The performance of keras-MLP is best at trim of 7 (with training accuracy of 97.6%). The best classifier for our data set is MLP (as shown in Table 2), while the QDA got the lowest score since it has shown highest difference between training and validation curves.

The GUI shown in Figure 7 shows a maximum scalograms (image) size of 1500×300 pixels, which can be optimised to increase accuracy and reduce training time. The performance of the Wavelet scalograms classifier where CNN varies with respect to the resize value (from 18% up to 70%, as is shown in Figure 9. The trim period between 18% and 70% was chosen with respect to the processing resources and time for the raspberry pi 4 and to correctly fit into the designed deep CNN learning model. The performance of the scalograms CNN classifier is best with trimming of 2 (EGG data size of 6 seconds) and resize of 22%, which corresponds to image size 330×66 pixels (rgb mode). The training duration of CNN with scalograms is greater than 24 hours when the scale of scalograms is around 70% without trimming the raw EEG data. The optimal trimming value of 2 is inferred from Figure 10 for both rgb and grayscale modes. We conclude that the performance of CNN with scalograms degrades when the trimming and scalograms sizes are increased, which is typical for deep learning algorithms that

Multi-Knowledge Electronic Comprehensive Journal For
Education And Science Publications (MECSJ)
Issue (50) 2022
ISSN: 2616-9185
www.mecsj.com

Table 2: Performance scores for 1-D and scalograms classifiers.

Classifier	Trim (s)	Average accuracy %		Resize %	Performance score
		Train	Test		
QDA	7	97	86	-	■□□□□□ (least)
NB	4	94	93	-	■■■■■□
MLP (sKlearn)	4	95	95	-	■■■■■■ (best)
LDA	4	95	98	-	■■■■□□
Keras-MLP	7	98	88	-	■■□□□□
Scalograms CNN	2	98	100	22	■■■□□□

necessitate great number of EEG data. A summary of performance results is shown in Table 2.

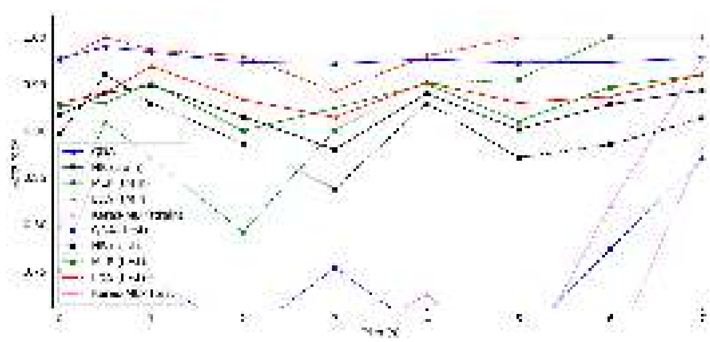

Figure 8: 1-D Wavelet classifiers average accuracies vs. trim (EEG data length).

Deep learning models, such as MLP and scalograms CNN produce high training and testing accuracies, they require careful tuning, considerable number of training epochs and processing resources. Therefore, LDA and NB for instance become handy to test the EEG data set for convergence and fast predictions.

Once trained and saved, desired machine learning models can be selected through the GUI in order to be used for classification of new EEG input during normal operation of the prostheses.

5 Conclusion

Prosthetic control using Wavelet EEG features is an essential field of scientific research that brought enormous benefits to health, economy, industry and community.

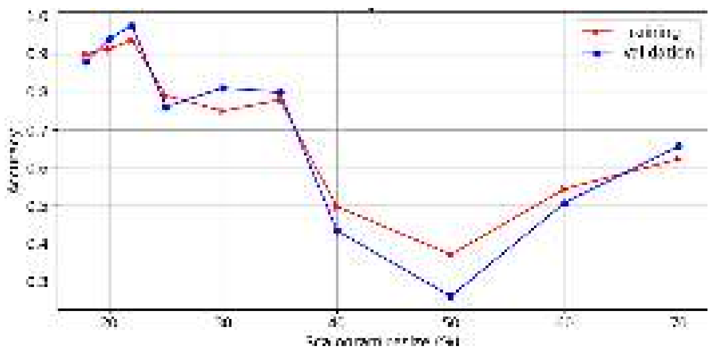

Figure 9: Effect of resizing scalograms in Wavelet classifiers.

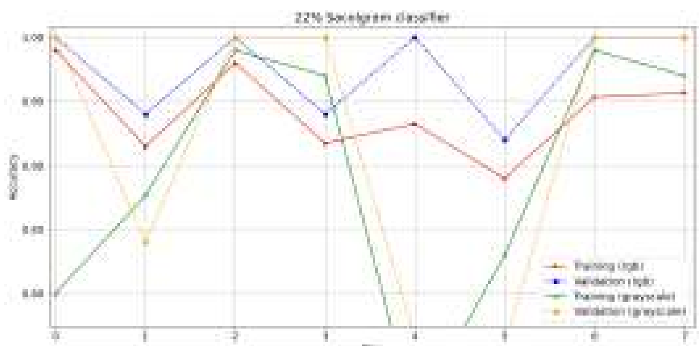

Figure 10: Trim effect on scalograms CNN (resized at 22%).

Electroencephalogram (EEG) is a technology that records the electrical signal activity of the brain, which varies with physical activity and thinking. Wavelets features and EEG are the basis of many BCI applications, where electrical brain waves are captured, filtered, converted to digital form and classified using various machine-learning algorithms.

In this work, we evaluated the performance of four 1-D and 1 scalograms Wavelet EEG classifiers for optimal prosthetic control that is beneficial for individuals suffering from severe motor disabilities, where control of prosthetic arm may be achieved by brain signals.

The designed optimised prosthetic arm control system is based upon a dual-channel EEG acquisition module and several machine learning algorithms including NB, MLP, LDA and scalograms CNN. We have provided thorough comparison between 1-D and scalograms in terms of performance parameters relevant to EEG input duration and size of scalograms. The training is based upon local EEG data set, which contains 184 classes recorded for 7 subjects. The complete system is compact and hosted in a raspberry pi 4 with sufficient processing power including 8 GB memory, which is enough to perform DSP, training and PWM control necessary to control the servomotors inside the prosthetic arm.

The results of performance evaluation indicate that 1-D EEG Wavelet classifiers are more advantageous compared to scalograms in terms of optimal length of EEG data (higher trimming), i.e., EEG length could be reduced to 4 seconds instead of full 8 seconds of the original raw EEG data. On the other hand, scalograms CNN classifier and produced highest training accuracy of 99% when trimming was 2 seconds.

The advantages of the designed system include compact design, moderate-training times, wide bandwidth covering frequencies from 0.2 up to 500 Hz, flexible scalograms resize parameter that can be selected prior to training, dual channel EEG acquisition with 2 kHz sampling frequency, simplicity, compactness and low cost.

The future work relevant to this work include fine tuning of the deep learning classifier models to improve EEG pre-processing, training time, responsiveness of the prosthetic control system and decrease over fitting through investigating different Wavelet functions.

Declaration of competing interest / Conflict of interest

The authors declare that they have no known competing financial interests or personal relationships that could have appeared to influence the work reported in this paper.

References

[1] Abdulkader, S.N., Atia, A., Mostafa, M.S.M., 2015. Brain computer interfacing: Applications and challenges. Egyptian Informatics Journal 16, 213–230. URL: https://www.sciencedirect.com/science/article/pii/S1110866515000237, doi:https://doi.org/10.1016/j.eij.2015.06.002.

[2] Al-Canaan, A., Uzair., M., 2020. Dual-Channel EEG Acquisition Circuit for Vehicular Safety System Based upon Brain-Computer Interface (BCI). The Journal of Engineering, Science and Computing (JESC) 2.

[3] Andrianesis, K., Tzes, A., 2015. Development and Control of a Multifunctional Prosthetic Hand with Shape Memory Alloy Actuators. Journal of Intelligent and Robotic Systems: Theory and Applications 78, 257–289. doi:10.1007/s10846-014-0061-6.

[4] Bajaj, N., 2021. Wavelets for EEG Analysis, in: Mohammady, S. (Ed.), Wavelet Theory. IntechOpen, Rijeka. chapter 5. URL: https://doi.org/10.5772/intechopen.94398, doi:10.5772/intechopen.94398.

[5] Barbosa, A., Achanccaray, D., Meggiolaro, M., 2010. Activation of a Mobile Robot Through a Brain-Computer Interface, in: IEEE International Conference on Robotics and Automation (ICRA).

[6] Bird, J.J., Faria, D.R., Manso, L.J., Ayrosa, P.P.S., Ekárt, A., 2021. A study on CNN image classification of EEG signals represented in 2D and 3D. Journal of Neural Engineering 18, 026005. doi:10.1088/1741-2552/abda0c.

[7] Bird, J.J., Pritchard, M., Fratini, A., Ekárt, A., Faria, D.R., 2021. Synthetic Biological Signals Machine-Generated by GPT-2 Improve the Classification of EEG and EMG Through Data Augmentation. IEEE Robotics and Automation Letters 6, 3498–3504. doi:10.1109/LRA.2021.3056355.

[8] Brumberg, J., Nieto-Castanon, A., Kennedy, P., Guenther, F., 2010. Brain-Computer Interfaces for Speech Communication. Speech Communication 52, 367–379.

[9] Chin, C., Bor-Shyn, L., Fu-Chuang, L., Che-Jui, 2014. Brain Computer Interface-Based Smart Living Environment Auto-Adjustment System in UPnP Home Networking. IEEE Systems Journal 8, 363–370.

[10] Desai, R., Porob, P., Rebelo, P., Edla, D.R., Bablani, A., 2020. EEG Data Classification for Mental State Analysis Using Wavelet Packet Transform and Gaussian Process Classifier. Wireless Personal Communications URL: https://doi.org/10.1007/s11277-020-07675-7, doi:10.1007/s11277-020-07675-7.

[11] Digilent, I., . Electronics Explorer: All-in-one USB Oscilloscope, Multimeter and Workstation.

[12] Dong, Y., Hu, Z., Uchimura, K., Murayama, N., 2011. Driver Inattention Monitoring System for Intelligent Vehicles. Intelligent Transport Systems, IEEE Transactions 12, 594–614.

[13] Fadzal, C., Mansor, W., Khuan, L., 2011. Review of Brain Computer Interface Application in Diagnosing Dyslexia,, in: Control and System Graduate Research Colloquium (ICSGRC).

[14] Guntar, S., Clemens, E., Christoph, H., Mel, G., 2009. Brain-Computer Interfaces for Goal Oriented Control of a Virtual Smart Home Environment, in: 4th International IEEE/EMBS Conference on Neural Networks.

[15] Hamsa, S., Shahin, I., Iraqi, Y., Werghi, N., 2020. Emotion Recognition From Speech Using Wavelet Packet Transform Cochlear Filter Bank and Random Forest Classifier. IEEE Access, Access, IEEE 8, 96994–97006. URL: http://sdl.edu.sa/middleware/Default.aspx?USESDL=true&PublisherID=AllPublishers&BookURL=https://sdl.idm.oclc.org/login?url=http://search.ebscohost.com/login.aspx?direct=true&db=edseee&AN=edseee.9084091&site=eds-live.

[16] Hinrichs, H., Scholz, M., Baum, A.K., Kam, J.W.Y., Knight, R.T., Heinze, H.J., 2020. Comparison Between a Wireless Dry Electrode EEG System with a Conventional Wired Wet Electrode EEG System for Clinical Applications. Scientific Reports 10.

[17] Hirra, I., Ahmad, M., Hussain, A., Ashraf, M.U., Saeed, I.A., Qadri, S.F., Alghamdi, A.M., Alfakeeh, A.S., 2021. Breast Cancer Classification From Histopathological Images Using Patch-Based Deep Learning Modeling. IEEE Access 9, 24273–24287. doi:10.1109/ACCESS.2021.3056516.

[18] Katie, Z., Nicolas, S., Vincent, M., Saurav, A., Emanuele, F., Edoardo, D., Fiorenzo, A., Francesco, P., Giuseppe, G., Giovanni, C., Wassim, R., Aude, B., Silvestro, M., 2019. Shared Human-robot Proportional Control of a Dexterous Myoelectric Prosthesis. Nature Machine Intelligence 1, 400–411. URL: https://doi.org/10.1038/s42256-019-0093-5, doi:10.1038/s42256-019-0093-5.

[19] Krasoulis, A., Kyranou, I., Erden, M.S., Nazarpour, K., Vijayakumar, S., 2017. Improved prosthetic hand control with concurrent use of myoelectric and inertial measurements. Journal of NeuroEngineering and Rehabilitation 14, 71. URL: https://doi.org/10.1186/s12984-017-0284-4, doi:10.1186/s12984-017-0284-4.

[20] LANGEVIN, G., 2021. InMoov: Open-Source 3D-Printed Life-size Robot. URL: http://inmoov.fr/inmoov-prosthetic-hand-almost-ready/.

[21] Lelievre, Y., Washizawa, Y., Rutkowski, T.M., 2013. Single Trial BCI Classification Accuracy Improvement for the Novel Virtual Sound Movement-based Spatial Auditory Paradigm, in: Proceedings of the Fifth APSIPA Annual Summit and Conference (APSIPA ASC 2013).

[22] Meng, J., Zhang, S., Bekyo, A., Olsoe, J., Baxter, B., He, B., 2016. Noninvasive Electroencephalogram Based Control of a Robotic Arm for Reach and Grasp Tasks. Scientific Reports 6, 38565. URL: https://doi.org/10.1038/srep38565, doi:10.1038/srep38565.

[23] Mohammadi, A., Lavranos, J., Zhou, H., Mutlu, R., Alici, G., Tan, Y., Choong, P., Oetomo, D., 2020. A practical 3D-Printed Soft Robotic Prosthetic Hand with Multi-articulating Capabilities. PLOS ONE 15, 1–23. URL: https://doi.org/10.1371/journal.pone.0232766, doi:10.1371/journal.pone.0232766.

[24] Ou, C.Z., Lin, B.S., Chang, C.J., Lin, C.T., 2012. Brain Computer Interface-based Smart Environmental Control System, in: Eighth International Conference on Intelligent Information Hiding and Multimedia Signal Processing (IIHMSP).

[25] Pei, G., Wu, J., Chen, D., Guo, G., Liu, S., Yan, M.H.T., 2018. Effects of an Integrated Neurofeedback System with Dry Electrodes: EEG Acquisition and Cognition Assessment,. Sensors 18, 3396.

[26] Rao, S.R., 2010. Brain-computer interfacing [in the spotlight]. Signal Process Mag, IEEE, 27, 150–152.

[27] Selvam, V., Shenbagadevi, S., 2011. Brain Tumor Detection Using Scalp EEG with Modified Wavelet-ICA and Multi-layer Feed Forward Neural Network. Engineering in Medicine and Biology Society, EMBC .

[28] Sharanreddy, M., Kulkarni, P., 2013. Detection of Primary Brain Tumor Present in EEG Signal Using Wavelet Transform and Neural Network. International Journal of Biological and Medical Research 4.

[29] Sharif, M., Erdoğmuş, D., Padir, T., 2019. Human-in-the-Loop Prosthetic Robot Hand Control Using Particle Filters for Grasp Selection, in: Third IEEE International Conference on Robotic Computing (IRC).

[30] Tan, D.S., Nijholt, A. (Eds.), 2010. Brain-Computer Interfaces and Human-Computer Interaction. Springer London, London. pp. 3–19. URL: https://doi.org/10.1007/978-1-84996-272-8_1, doi:10.1007/978-1-84996-272-8_1.

[31] Tee, Y.W., Siti, A.M.A., 2020. Electroencephalogram (EEG) Stress Analysis on Alpha/Beta Ratio and Theta/Beta Ratio. Indonesian Journal of Electrical Engineering and Computer Science 17, 175–182. doi:10.11591/ijeecs.v17.i1.

[32] Van Erp, J., Lotte, F., Tangermann, M., 2012. Brain-computer interfaces: beyond medical applications. Computer 45, 150–152.

[33] Vourvopoulos, A., Liarokapis, F., 2012. Robot Navigation using Brain-Computer Interfaces, in: EEE 11th International Conference on Trust, Security and Privacy in Computing and Communications (TrustCom),.

[34] Wang, W., Degenhart, A., Sudre, G., Pomerleau, D., Tyler-Kabara, E., 2011. Decoding Semantic Information from Human Electrocorticographic (ECOG) Signals, in: Engineering in Medicine and Biology Society, EMBC, Annual International Conference of the IEEE.

[35] Zhaolong, G., Rongyu, T., Luyao, C., Qiang, H., Jiping, H., 2020. Continuous Shared Control in Prosthetic Hand Grasp Tasks by Deep Deterministic Policy Gradient with Hindsight Experience Replay. International Journal of Advanced Robotic Systems 17, 1729881420936851. URL: https://doi.org/10.1177/1729881420936851, doi:10.1177/1729881420936851, arXiv:https://doi.org/10.1177/1729881420936851.